

Extraordinary-log surface phase transition in the three-dimensional XY model

Minghui Hu,¹ Youjin Deng,^{2,3,*} and Jian-Ping Lv^{1,†}

¹*Department of Physics and Anhui Key Laboratory of Optoelectric Materials Science and Technology, Key Laboratory of Functional Molecular Solids, Ministry of Education, Anhui Normal University, Wuhu, Anhui 241000, China*

²*Hefei National Laboratory for Physical Sciences at Microscale and Department of Modern Physics, University of Science and Technology of China, Hefei, Anhui 230026, China*

³*MinJiang Collaborative Center for Theoretical Physics, College of Physics and Electronic Information Engineering, Minjiang University, Fuzhou 350108, China*

(Dated: July 18, 2022)

Critical universality classes are ubiquitous in nature. The standard scenario is that the two-point correlation algebraically decreases with the distance r as $g(r) \asymp r^{2-d-\eta}$ (d is spatial dimensionality). Recently, an unusual logarithmic universality was put forward to describe the extraordinary surface transition of three-dimensional $O(N)$ critical systems, which has long been theoretically debated. In this logarithmic universality, $g(r)$ decays in a power of logarithmic distance as $g(r) \asymp [\ln(r)]^{-\eta}$, dramatically different from the standard scenario. We explore the three-dimensional XY model by extensive Monte Carlo simulations, and provide strong evidence for the emergence of logarithmic universality. Moreover, on the basis of our simulations, we propose that the finite-size scaling of $g(r, L)$ is described by an ansatz simultaneously containing the r -dependent term $g(r) \asymp [\ln(r)]^{-\eta'}$ as well as an r -independent plateau at large distance whose height decays logarithmically with L as $g(r) \asymp [\ln(L)]^{-\eta}$. These results expand our understanding of critical universality classes.

Keywords: surface critical behavior; extraordinary-log transition; $O(N)$ model; universality class

Introduction. Surface critical behavior (SCB) refers to the critical phenomena occurring on the boundaries of a critical bulk. From the viewpoint of the renormalization group (RG), surface fixed point in presence of a critical bulk is not necessarily unique, hence rich SCB may emerge. The topic has been long-standing and fascinated physicists for decades, ever since Binder in 1970s [1–10]. Renewed interest originated from the symmetric protected topological phases with exotic surface effects, of which some could be explained in the context of SCB [11–15].

The $O(N)$ model includes the well-known limits $N = 0$ (self-avoiding random walk), 1 (Ising model), 2 (XY model) and 3 (Heisenberg model). Meanwhile, an $O(N)$ criticality in d -dimensional classical system can be related to its counterpart in $(d-1)$ -dimensional quantum system due to classical-quantum mapping. As a result, the $O(N)$ criticality has tremendous realizations [16–18].

The $O(N)$ model exhibits rich SCB including the *special*, *ordinary*, and *extraordinary* transitions, depending on N and d [1–10]. The $d = 3$ situations are no doubt practically relevant. However, they are extremely subtle and require case-by-case analyses [6–10].

Recently, the logarithmic universality of the extraordinary transition was put forward for the three-dimensional $O(N)$ model with $2 \leq N < N_c$ by means of RG [8], where N_c is not exactly known. It was predicted that the two-point correlation $g(r) \equiv \langle \vec{S}_0 \cdot \vec{S}_r \rangle$ on surface decays logarithmically with the distance r as [8]

$$g(r) \asymp [\ln(r/r_0)]^{-\hat{\eta}}, \quad (1)$$

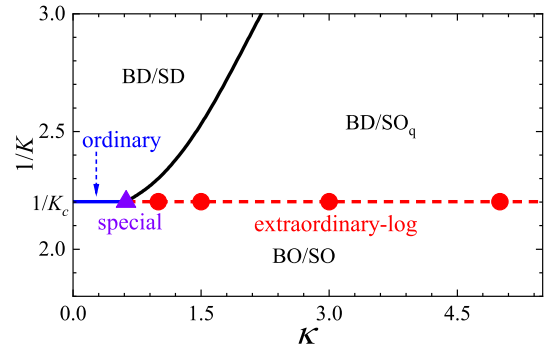


Figure 1. Phase diagram of the XY model (2). The horizontal axis is for the surface coupling enhancement κ and the vertical axis relates to the bulk coupling K by $1/K$. Phases are denoted by the abbreviations BD (bulk disorder), BO (bulk order), SD (surface disorder), SO_q (surface quasi-long-range order), and SO (surface order). The ordinary, the extraordinary-log, and the SD- SO_q critical lines meet together at the special critical point. Parameters denoted by red cycles are used in this work to analyze the extraordinary-log universal class.

where r_0 is a non-universal constant. If N is specified, the critical exponent $\hat{\eta}$ is universal in extraordinary regime. This form is drastically different from the standard scenario $g(r) \asymp r^{2-d-\eta}$, with η the anomalous dimension. A quantum Monte Carlo study has been performed for the SCB of $(2+1)$ -dimensional $O(3)$ universality in a two-dimensional dimerized quantum Heisenberg model [9]. However, both the logarithmic and the extraordinary-power behavior [8] were not observed. By contrast, compelling evidence for the logarithmic universality was obtained from a classical $O(3)$ ϕ^4 model [10].

Motivated by the recent advances [8–10], we address the extraordinary-log universality in the context of $N = 2$.

* yjdeng@ustc.edu.cn

† jplv2014@ahnu.edu.cn

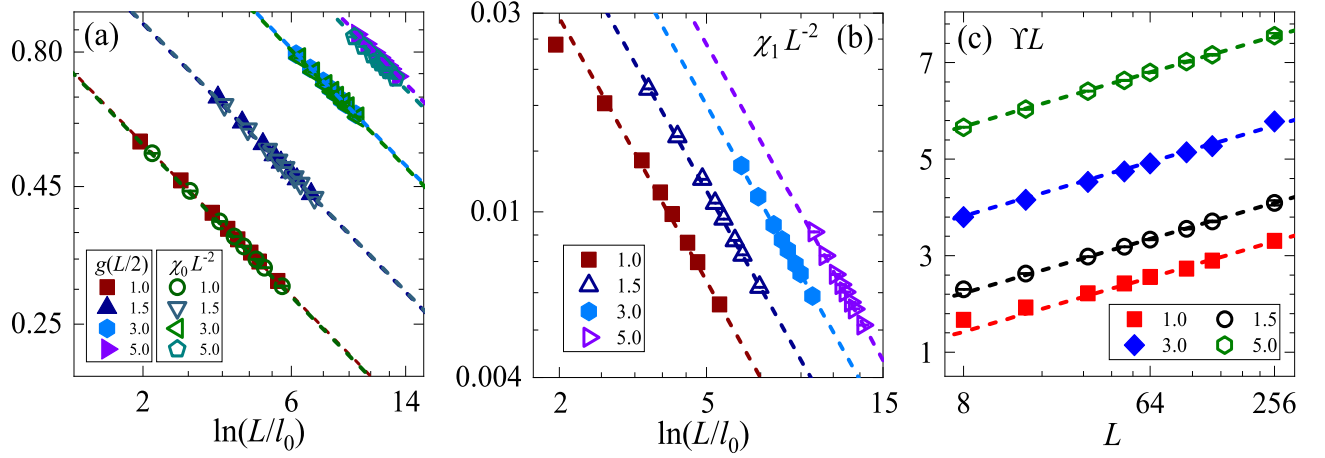


Figure 2. Results for the extraordinary-log transitions at $\kappa = 1, 1.5, 3$, and 5 . (a) Log-log plot of the two-point correlation $g(L/2)$ and the scaled susceptibility $\chi_0 L^{-2}$ versus $\ln(L/l_0)$. The parameter l_0 is κ -dependent and obtained from least-squares fits. Dashed lines have the slope -0.59 and denote the critical exponent $\hat{\eta} = 0.59(2)$. (b) Log-log plot of the scaled magnetic fluctuations $\chi_1 L^{-2}$ versus $\ln(L/l_0)$. Dashed lines have the slope -1.59 and denote the exponent $\hat{\eta}' \approx 1.59$. (c) Scaled helicity modulus ΥL versus L . The horizontal axis is in a log scale. Dashed lines have the slope 0.54 and relate to the universal RG parameter $\alpha = 0.27(2)$ by 2α .

Hence, if the RG prediction is correct, the logarithmic universality would emerge, regardless of the exact value of N_c . We consider the XY model on simple-cubic lattices with the Hamiltonian [3, 6]

$$\mathcal{H}/(k_B T) = - \sum_{\langle \mathbf{r}\mathbf{r}' \rangle} K_{\mathbf{r}\mathbf{r}'} \vec{S}_{\mathbf{r}} \cdot \vec{S}_{\mathbf{r}'}, \quad (2)$$

where $\vec{S}_{\mathbf{r}}$ represents the XY spin on site \mathbf{r} and $K_{\mathbf{r}\mathbf{r}'} > 0$ denotes the nearest-neighbor ferromagnetic coupling. We impose open boundary conditions in one direction and periodic boundary conditions in other directions, hence a pair of open surfaces are specified. We set $K_{\mathbf{r}\mathbf{r}'} = K'$ if \mathbf{r} and \mathbf{r}' are on the same surface and $K_{\mathbf{r}\mathbf{r}'} = K$ otherwise. The surface coupling enhancement κ is defined by $\kappa \equiv (K' - K)/K$.

Figure 1 shows the phase diagram of model (2), which contains a long-range-ordered surface phase in presence of ordered bulk, as well as a disordered surface phase and a critical quasi-long-range-ordered surface phase in presence of disordered bulk. The critical lines meet together at the special transition point. A characteristic feature for $N = 2$ is the existence of the quasi-long-range-ordered phase, which is absent in $N = 1$ and $N \geq 3$ situations.

Consider the quasi-long-range-ordered regime. As $K \rightarrow K_c^-$, several scenarios of SCB are possible, owing to divergent bulk correlations. One scenario is that the surface long-range order develops at K_c as a result of the effective interactions mediated by long-range bulk correlations. This scenario can not be precluded by the Mermin-Wagner theorem as the effective interactions could be long-ranged. A previous study revealed [6] that the Monte Carlo data restricting to $L \leq 95$ (L is linear size) are not sufficient to preclude either discontinuous or continuous surface transition across the extraordinary critical line; the former implies long-range surface order at K_c .

Summary of main findings. By extensive Monte Carlo simu-

lations, we confirm the emergence of logarithmic universality in model (2). As shown in Fig. 2(a), the L dependence of surface two-point correlation $g(L/2)$ obeys the scaling formula $g(L/2) \asymp [\ln(L/l_0)]^{-\hat{\eta}}$ with $\hat{\eta} = 0.59(2)$.

We analyze the surface magnetic fluctuations $\Gamma(\mathbf{k}) = L^2 \langle ||\vec{m}(\mathbf{k})||^2 \rangle$ with $\vec{m}(\mathbf{k}) = (1/L^2) \sum_{\mathbf{r}} \vec{S}_{\mathbf{r}} e^{i\mathbf{k}\cdot\mathbf{r}}$, where the summation runs over sites on surface and \mathbf{k} denotes a Fourier mode. As shown in Figs. 2(a) and (b), the magnetic fluctuations $\chi_0 = \Gamma(0, 0)$ (susceptibility) and $\chi_1 = \Gamma(2\pi/L, 0)$ have the distinct finite-size scaling (FSS) behavior $\chi_0 \asymp L^2 [\ln(L/l_0)]^{-\hat{\eta}}$ and $\chi_1 \asymp L^2 [\ln(L/l_0)]^{-\hat{\eta}'}$, with $\hat{\eta}' \approx \hat{\eta} + 1$. Motivated by these observations as well as the two-distance scenarios in high-dimensional $O(N)$ critical systems [19–23] and quantum deconfined criticality [24], we conjecture that the FSS of critical two-point correlation behaves as

$$g(r) \asymp \begin{cases} [\ln(r/r_0)]^{-\hat{\eta}'}, & \ln r \leq \mathcal{O}[(\ln L)^{\hat{\eta}/\hat{\eta}'}], \\ [\ln(L/l_0)]^{-\hat{\eta}}, & \ln r \geq \mathcal{O}[(\ln L)^{\hat{\eta}/\hat{\eta}'}], \end{cases} \quad (3)$$

where r_0 and l_0 are non-universal constants. By (3), we point out two coexisting features: the r -dependent behavior $[\ln(r/r_0)]^{-\hat{\eta}'}$ and the large-distance r -independent plateau $[\ln(L/l_0)]^{-\hat{\eta}}$. Equation (3) is a possible explanation for the numerical observations and compatible with the FSS of second-moment correlation length at the extraordinary transition of $O(3)$ model [10, 25]. Recently, a two-distance scenario was proposed for the two-point correlation of $O(n)$ model at a marginal situation (the upper critical dimensionality) [22] and confirmed conclusively by large-scale numerical simulations on hyper-cubic lattices up to 768^4 sites [23]. Notice that the open surfaces of model (2) are at the lower critical dimensionality ($d_s = 2$) and also belong to marginal situations.

We confirm the scaling relation between $\hat{\eta}$ and the RG parameter of helicity modulus. The helicity modulus Υ measures the response of a system to a twist in boundary conditions [26]. The definition is given in the Supplementary

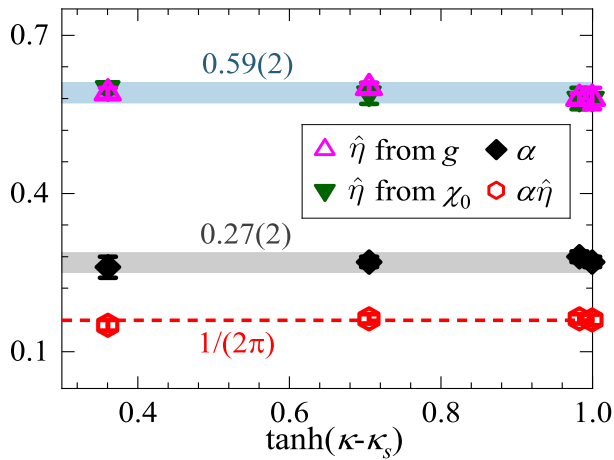


Figure 3. The critical exponent $\hat{\eta}$ estimated from $g(L/2)$ and χ_0 , the RG parameter α from Υ , and their product $\alpha\hat{\eta}$. The shadowed areas with 0.59(2) and 0.27(2) denote our final estimates of $\hat{\eta}$ and α , respectively. The red dashed line denotes the predicted value $\alpha\hat{\eta} = 1/(2\pi)$ by RG.

Materials (SM). Figure 2(c) demonstrates that Υ scales as $\Upsilon L \asymp 2\alpha \ln L$ with the RG parameter $\alpha = 0.27(2)$. As shown in Fig. 3, the universality of $\hat{\eta}$ and α are confirmed in an extensive domain of extraordinary regime. Finally, the scaling relation $\alpha\hat{\eta} = 1/(2\pi)$ is evidenced, conforming to the prediction [8]

$$\hat{\eta} = \frac{N-1}{2\pi\alpha}. \quad (4)$$

Technique aspects. To explore the SCB, we fix the bulk coupling strength at K_c . Hence a precise estimate of K_c would be a premise. Previously, two of us and coworkers performed extensive simulations utilizing the Prokof'ev-Svistunov worm algorithms [27, 28] on periodic simple-cubic lattices with $L_{\max} = 512$, and determined the critical bulk coupling K_c as $1/K_c = 2.2018441(5)$ [29]. This estimate was confirmed by an independent Monte Carlo study [30]. Here we simulate model (2) at $1/K_c = 2.2018441$ using Wolff's cluster algorithm [31] on L^3 simple-cubic lattices with $L_{\max} = 256$. We focus on the extraordinary transitions at $\kappa = 1, 1.5, 3$, and 5, and the special transition at $\kappa_s = 0.6222$ [6].

FSS will be performed by using least-squares fits. Following Refs. [30, 32], the fits are carried out by the function `curve_fit()` in `Scipy.library` with the default Levenberg-Marquardt algorithm. For caution, we compare the fits with the benchmarks obtained by implementing the Mathematica's `NonlinearModelFit` function as Ref. [33]. The fits with the Chi squared per degree of freedom $\chi^2/\text{DF} \sim 1$ are preferred. We do not trust any single fit and final conclusions are drawn based on comparing the fits that are stable against varying L_{\min} , the size of the minimum system incorporated.

Emergence of logarithmic universality. Figure 4(a) demonstrates the two-point correlation function $g(r)$ with $\kappa = 1$. The large-distance behavior can be monitored by the L dependence of $g(L/2)$. According to Eq. (1) or Eq. (3), we have

Table I. Estimates of the critical exponent $\hat{\eta}$ and the RG parameter α for $\kappa = 1$. $\hat{\eta}$ is estimated from the scaling formulae $g(L/2) \asymp [\ln(L/l_0)]^{-\hat{\eta}}$ and $\chi_0 \asymp [\ln(L/l_0)]^{-\hat{\eta}}$, and α is determined from $\Upsilon L = 2\alpha \ln L + A + BL^{-1}$.

	L_{\min}	χ^2/DF	$\hat{\eta}$ or α	l_0 or A
$g(L/2)$	16	2.91/4	0.596(2)	0.94(1)
	32	0.66/3	0.592(3)	0.97(2)
	48	0.58/2	0.591(5)	0.98(4)
χ_0	32	3.46/3	0.603(2)	1.13(2)
	48	0.08/2	0.598(4)	1.18(3)
	64	0.02/1	0.597(5)	1.19(5)
Υ	8	5.46/4	0.255(3)	0.41(2)
	16	3.33/3	0.265(7)	0.32(6)
	32	2.51/2	0.25(2)	0.4(2)

a scaling formula $g(L/2) \asymp [\ln(L/l_0)]^{-\hat{\eta}}$. We perform least-squares fits to this formula and obtain $\hat{\eta} = 0.596(2)$, $l_0 = 0.94(1)$, and $\chi^2/\text{DF} \approx 0.73$, with $L_{\min} = 16$. As L_{\min} is varied, preferred fits are also obtained (Table I). By comparing all these fits, our final estimate of $\hat{\eta}$ for $\kappa = 1$ is $\hat{\eta} = 0.59(1)$. In SM, we present similar analyses for $\kappa = 1.5, 3$ and 5, and the final estimates are $\hat{\eta} = 0.60(1)$ ($\kappa = 1.5$), $0.58(1)$ ($\kappa = 3$) and $0.58(2)$ ($\kappa = 5$). It is therefore confirmed that $g(L/2)$ obeys the logarithmic scaling $g(L/2) \asymp [\ln(L/l_0)]^{-\hat{\eta}}$, with a universal exponent $\hat{\eta} = 0.59(2)$.

Existence of two distinct exponents. For a conclusive verification of Eq. (3), we analyze the FSS of surface magnetic fluctuations. In the Monte Carlo simulations, we sample $\chi_2 = \Gamma(2\pi/L, 2\pi/L)$ as well as χ_0 and χ_1 .

According to (3), an r -independent plateau emerges at large distance. This plateau contributes to the magnetic fluctuations at zero mode but not to those at non-zero modes. The ratios χ_0/χ_1 at extraordinary transitions are shown in Fig. 4(b). As $L \rightarrow \infty$, the ratios keep increasing, implying distinct FSS of χ_0 and χ_1 .

More precisely, the susceptibility χ_0 at extraordinary transition is expected to scale as $\chi_0 \asymp L^2 [\ln(L/l_0)]^{-\hat{\eta}}$. The fits for $\kappa = 1$ are illustrated in Table I and those for $\kappa = 1.5, 3$, and 5 are given in SM. Comparing preferred fits, we obtain $\hat{\eta} = 0.60(1)$ ($\kappa = 1$), $0.59(2)$ ($\kappa = 1.5$), $0.58(2)$ ($\kappa = 3$), and $0.58(1)$ ($\kappa = 5$). These results are consistent with the exponents determined from the L dependence of $g(L/2)$ and confirm the final estimate $\hat{\eta} = 0.59(2)$.

We analyze the magnetic fluctuations χ_1 and χ_2 at nonzero Fourier modes by performing fits to $\chi_{\mathbf{k} \neq 0} \asymp L^2 [\ln(L/l_0)]^{-\hat{\eta}'}$. We confirm the fast decay of $\chi_1 L^{-2}$ and $\chi_2 L^{-2}$ with $\ln L$. As $\hat{\eta}'$ is large, it is difficult to give a precise estimate. For reducing uncertainties, we fix l_0 to those obtained from the scaling analyses of χ_0 , and estimate $\hat{\eta}' \approx 1.7$ over $\kappa = 1, 1.5, 3$, and 5. From the log-log plot of $\chi_1 L^{-2}$ versus $\ln(L/l_0)$ in Fig. 2(b), it is seen that the data nearly scale as $\chi_1 L^{-2} \asymp [\ln(L/l_0)]^{-\hat{\eta}'}$ with $\hat{\eta}' \approx 1.59$. Similar result is obtained for $\chi_2 L^{-2}$ (SM). Hence, the magnetic fluctuations χ_1 and χ_2

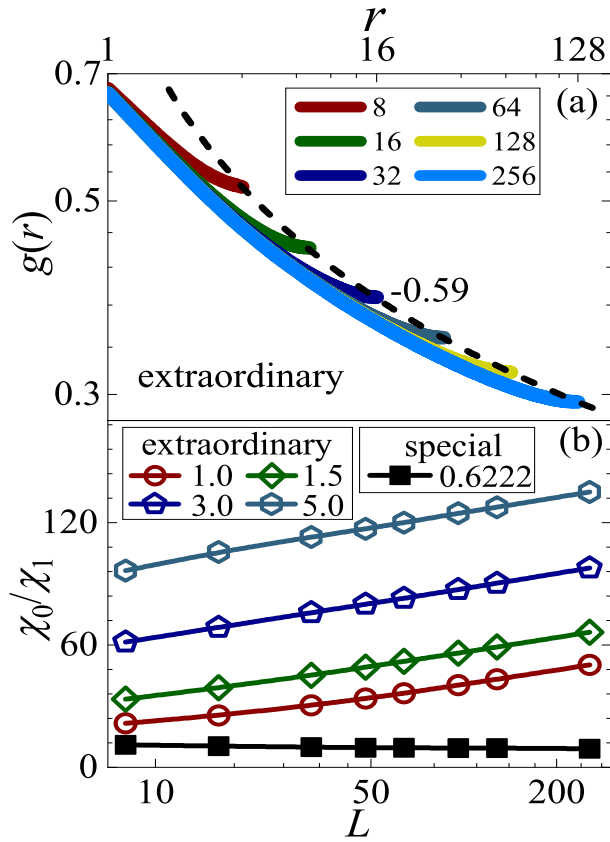


Figure 4. (a) The two-point correlation $g(r)$ for the extraordinary transition at $\kappa = 1$ with $L = 8, 16, 32, 64, 128,$ and 256 . The dashed line denotes the logarithmic decaying $[\ln(L/l_0)]^{-0.59}$ in the large-distance limit. (b) The ratio χ_0/χ_1 of magnetic fluctuations versus L for the extraordinary transitions at $\kappa = 1, 1.5, 3,$ and $5,$ and for the special transition at $\kappa_s = 0.6222$.

obey the logarithmic FSS formula $\chi_{k \neq 0} \asymp L^2 [\ln(L/l_0)]^{-\hat{\eta}'}$, with $\hat{\eta}' \approx 1.6$.

Our observations for the FSS of magnetic fluctuations χ_0 and χ_1 are compatible with the Monte Carlo data [10, 25] of the second-moment correlation length ξ_{2nd} , which scales as $(\xi_{2nd}/L)^2 \asymp (\chi_0/\chi_1 - 1) \asymp \ln L$. The relation $\hat{\eta}' = \hat{\eta} + 1$ is implied.

As $\hat{\eta}'$ is much larger than $\hat{\eta}$, the two-distance scenario (3) indicates that the r -dependent contribution decays fast. This explains the profile of $g(r)$ in Fig. 4(a), where the large-distance plateau soon dominates as $L \rightarrow \infty$.

By contrast, the special transition belongs to the standard scenario of continuous transition. In the standard scenario, the r -dependent behavior converges to the power law $g(r) \asymp r^{-\eta}$, which is comparable with the contribution from $g(L/2) \asymp L^{-\eta}$. Moreover, the magnetic renormalization exponent y_h relates to the anomalous dimension η by $y_h = (2 - \eta + d_s)/2$, and the magnetic fluctuations $\chi_0, \chi_1,$ and χ_2 all scale as $L^{2y_h - 2}$. As shown in Fig. 4(b), the ratio χ_0/χ_1 converges fast to a constant upon increasing L . More results for $g(r), \chi_0, \chi_1$ and χ_2 at the special transition are given in SM.

Scaling relation. The helicity modulus Υ , also known as

spin-wave stiffness, measures the response of a system to a twist in boundary conditions [26]. It was predicted [8, 25] that ΥL diverges logarithmically as $\Upsilon L \asymp 2\alpha \ln L$, with α a universal RG parameter. Further, the universal scaling relation (4) between α and $\hat{\eta}$ was established [8]. These predictions are supported by the Monte Carlo results of an $O(3)$ ϕ^4 model [10].

We sample Υ of model (2) by Monte Carlo simulations. The dependence of ΥL with $\ln L$ is shown in Fig. 2(c) for $\kappa = 1, 1.5, 3,$ and 5 . For each κ , a nearly linear relation in large- L regime is observed. Further, we perform a FSS analysis of Υ according to $\Upsilon L = 2\alpha \ln L + A + BL^{-1}$, where A and B are constants. We explore the situations with and without the correction term BL^{-1} separately. Stable fits are obtained, and final estimates are $\alpha = 0.26(2)$ ($\kappa = 1$), $0.27(1)$ ($\kappa = 1.5$), $0.28(1)$ ($\kappa = 3$), and $0.27(1)$ ($\kappa = 5$). Comparing these estimates, the universal value of α is determined as $\alpha = 0.27(2)$. As shown in Fig. 3, the scaling relation (4) is confirmed.

Discussions. By means of extensive simulations, we study the SCB of the three-dimensional XY model, paying particular attention to the extraordinary transition. We obtain conclusive evidence for the emergence of extraordinary-log universality class, predicted recently for the $O(N)$ criticality [8]. Further, we propose a two-distance scenario for the extraordinary-log universality by Eq. (3) and show that the Monte Carlo data can be described by the scenario.

A variety of open questions arise. First, here we demonstrate essentially that a two-dimensional XY system with *finely tuned* long-range interactions exhibits an unusual logarithmic universality. Is it possible to formulate the interactions in a microscopic Hamiltonian? Second, the existence of the extraordinary-log transition has also been demonstrated in a Heisenberg model [10]. Hence, it is promising to verify the two-distance scenario for the $N = 3$ case, which might be applicable to explaining the exotic surface correlations in quantum $O(3)$ systems such like the dimerized Heisenberg model [9, 14, 15]. Finally, the two-distance scenario is reminiscent of that for the upper-critical-dimensional $O(n)$ models, where the short-distance behavior is dominated by Gaussian fixed point and an r -independent finite-size plateau emerges at large distance [22]. The introduction of unwrapped distance plays a central role in the verification of two-distance scenario [23]. A future direction is to sample the unwrapped distance for model (2).

ACKNOWLEDGMENTS

We thank Max Metlitski for useful discussions and comments. This work has been supported by the National Natural Science Foundation of China (under Grant Nos. 11774002, 11625522, and 11975024), the Science and Technology Committee of Shanghai (under grant No. 20DZ2210100), the National Key R&D Program of China (under Grant No. 2018YFA0306501), and the Education Department of Anhui.

-
- [1] K Binder and P. C. Hohenberg, “Surface effects on magnetic phase transitions,” *Phys. Rev. B* **9**, 2194 (1974).
- [2] K. Ohno and Y. Okabe, “The $1/n$ expansion for the extraordinary transition of semi-infinite system,” *Prog. Theor. Phys.* **72**, 736–745 (1984).
- [3] D. P. Landau, R. Pandey, and K. Binder, “Monte carlo study of surface critical behavior in the xy model,” *Phys. Rev. B* **39**, 12302 (1989).
- [4] H. W. Diehl, “The theory of boundary critical phenomena,” *Int. J. Mod. Phys. B* **11**, 3503–3523 (1997), [arXiv:cond-mat/9610143 \[cond-mat\]](#).
- [5] M. Pleimling, “Critical phenomena at perfect and non-perfect surfaces,” *J. Phys. A: Math. and Gen.* **37**, R79 (2004), [arXiv:cond-mat/0402574 \[cond-mat\]](#).
- [6] Y. Deng, H. W. J. Blöte, and M. P. Nightingale, “Surface and bulk transitions in three-dimensional $o(n)$ models,” *Phys. Rev. E* **72**, 016128 (2005), [arXiv:cond-mat/0504173 \[cond-mat\]](#).
- [7] Y. Deng, “Bulk and surface phase transitions in the three-dimensional $o(4)$ spin model,” *Phys. Rev. E* **73**, 056116 (2006).
- [8] M. A. Metlitski, “Boundary criticality of the $o(n)$ model in $d=3$ critically revisited,” [arXiv:2009.05119 \[cond-mat\]](#).
- [9] L. Weber and S. Wessel, “Spin versus bond correlations along dangling edges of quantum critical magnets,” *Phys. Rev. B* **103**, L020406 (2021), [arXiv:2010.15691 \[cond-mat\]](#).
- [10] F. Parisen Toldin, “Boundary critical behavior of the three-dimensional heisenberg universality class,” *Phys. Rev. Lett.* **126**, 135701 (2021), [arXiv:2012.00039 \[cond-mat\]](#).
- [11] T. Grover and A. Vishwanath, “Quantum criticality in topological insulators and superconductors: Emergence of strongly coupled majoranas and supersymmetry,” [arXiv:1206.1332 \[cond-mat\]](#).
- [12] D. E. Parker, T. Scaffidi, and R. Vasseur, “Topological luttinger liquids from decorated domain walls,” *Phys. Rev. B* **97**, 165114 (2018), [arXiv:1711.09106 \[cond-mat\]](#).
- [13] L. Zhang and F. Wang, “Unconventional surface critical behavior induced by a quantum phase transition from the two-dimensional affleck-kennedy-lieb-tasaki phase to a néel-ordered phase,” *Phys. Rev. Lett.* **118**, 087201 (2017), [arXiv:1611.06477 \[cond-mat\]](#).
- [14] C. Ding, L. Zhang, and W. Guo, “Engineering surface critical behavior of $(2+1)$ -dimensional $o(3)$ quantum critical points,” *Phys. Rev. Lett.* **120**, 235701 (2018), [arXiv:1801.10035 \[cond-mat\]](#).
- [15] L. Weber, F. Parisen Toldin, and S. Wessel, “Nonordinary edge criticality of two-dimensional quantum critical magnets,” *Phys. Rev. B* **98**, 140403(R) (2018), [arXiv:1804.06820 \[cond-mat\]](#).
- [16] R. Fernández, J. Fröhlich, and A. D. Sokal, *Random walks, critical phenomena, and triviality in quantum field theory* (Springer, Berlin, 2013).
- [17] A. Goldman, *Percolation, localization, and superconductivity*, Vol. 109 (Springer, Boston, 2013).
- [18] B. V. Svistunov, E. S. Babaev, and N. V. Prokof’ev, *Superfluid states of matter* (CRC Press, London, 2015).
- [19] V. Papanthakos, *Finite-size effects in high-dimensional statistical mechanical systems: The Ising model with periodic boundary conditions* (Ph.D. thesis, Princeton University, Princeton, New Jersey, 2006).
- [20] J. Grimm, E. M. Elçi, Z. Zhou, T. M. Garoni, and Y. Deng, “Geometric explanation of anomalous finite-size scaling in high dimensions,” *Phys. Rev. Lett.* **118**, 115701 (2017), [arXiv:1612.01722 \[cond-mat\]](#).
- [21] Z. Zhou, J. Grimm, S. Fang, Y. Deng, and T. M. Garoni, “Random-length random walks and finite-size scaling in high dimensions,” *Phys. Rev. Lett.* **121**, 185701 (2018), [arXiv:1809.00515 \[cond-mat\]](#).
- [22] J.-P. Lv, W. Xu, Y. Sun, K. Chen, and Y. Deng, “Finite-size scaling of $o(n)$ systems at the upper critical dimensionality,” *Nat. Sci. Rev.* **8**, nwaa212 (2021), [arXiv:1909.10347 \[cond-mat\]](#).
- [23] S. Fang, Y. Deng, and Z. Zhou, “Logarithmic finite-size scaling of the self-avoiding walk at four dimensions,” [arXiv:2103.04340 \[cond-mat\]](#).
- [24] H. Shao, W. Guo, and A. W. Sandvik, “Quantum criticality with two length scales,” *Science* **352**, 213–216 (2016), [arXiv:1603.02171 \[cond-mat\]](#).
- [25] M. A. Metlitski, *Finite size corrections in the extra-ordinary log phase* (Private Communication, 2021).
- [26] M. E. Fisher, M. N. Barber, and D. Jasnow, “Helicity modulus, superfluidity, and scaling in isotropic systems,” *Phys. Rev. A* **8**, 1111–1124 (1973).
- [27] N. V. Prokof’ev and B. V. Svistunov, “Worm algorithms for classical statistical models,” *Phys. Rev. Lett.* **87**, 160601 (2001), [arXiv:cond-mat/0103146 \[cond-mat\]](#).
- [28] N. V. Prokof’ev and B. V. Svistunov, “Worm algorithm for problems of quantum and classical statistics,” in *Understanding Quantum Phase Transitions* (2010) pp. 499–522, [arXiv:0910.1393 \[cond-mat\]](#).
- [29] W. Xu, Y. Sun, J.-P. Lv, and Y. Deng, “High-precision monte carlo study of several models in the three-dimensional $u(1)$ universality class,” *Phys. Rev. B* **100**, 064525 (2019), [arXiv:1908.10990 \[cond-mat\]](#).
- [30] M. Hasenbusch, “Monte carlo study of an improved clock model in three dimensions,” *Phys. Rev. B* **100**, 224517 (2019), [arXiv:1910.05916 \[cond-mat\]](#).
- [31] U. Wolff, “Collective monte carlo updating for spin systems,” *Phys. Rev. Lett.* **62**, 361 (1989).
- [32] M. Hasenbusch, “Monte carlo study of a generalized icosahedral model on the simple cubic lattice,” *Phys. Rev. B* **102**, 024406 (2020), [arXiv:2005.04448 \[cond-mat\]](#).
- [33] J. Salas, “Phase diagram for the bisected-hexagonal-lattice five-state potts antiferromagnet,” *Phys. Rev. E* **102**, 032124 (2020), [arXiv:2006.04866 \[cond-mat\]](#).

Supplementary Materials for: “Extraordinary-log surface phase transition in the three-dimensional XY model”

Minghui Hu,¹ Youjin Deng,^{2,3,*} and Jian-Ping Lv^{1,†}

¹*Department of Physics and Anhui Key Laboratory of Optoelectric Materials Science and Technology,
Key Laboratory of Functional Molecular Solids, Ministry of Education,
Anhui Normal University, Wuhu, Anhui 241000, China*

²*Hefei National Laboratory for Physical Sciences at Microscale and Department of Modern Physics,
University of Science and Technology of China, Hefei, Anhui 230026, China*

³*MinJiang Collaborative Center for Theoretical Physics,
College of Physics and Electronic Information Engineering, Minjiang University, Fuzhou 350108, China*
(Dated: July 18, 2022)

In this Supplementary Materials (SM), we present more details on the finite-size scaling (FSS) of the extraordinary-log transition and the special transition.

I. EXTRAORDINARY-LOG TRANSITION

For exploring the extraordinary transition, we consider the surface coupling enhancements $\kappa = 1, 1.5, 3$ and 5 .

The two-point correlation function $g(r)$ for $\kappa = 1$ has been shown in Fig. 4(a) of the main text. In this SM, we present the results for $\kappa = 1.5, 3$ and 5 in Fig. 1, with $L_{\max} = 256$. We fit the $g(L/2)$ data to the ansatz

$$g(L/2) = A[\ln(L/l_0)]^{-\hat{\eta}}, \quad (1)$$

where $\hat{\eta}$ is a universal exponent. A and l_0 are non-universal constants. The results for the fits are given in Table I. We evaluate the uncertainties of fits by incorporating both statistical and systematic errors. The latter is estimated by examining the stability of fits against varying L_{\min} . By comparing the estimates for considered enhancements, our final result of $\hat{\eta}$ is $\hat{\eta} = 0.59(2)$.

The FSS of the susceptibility χ_0 is shown in Fig. 2(a) of the main text. We analyze the critical susceptibility with the scaling formula

$$\chi_0 = AL^2[\ln(L/l_0)]^{-\hat{\eta}}. \quad (2)$$

The details of fits are given in Table II. The result $\hat{\eta} = 0.59(2)$ is confirmed.

For χ_1 and χ_2 , we perform fits to the scaling formula

$$\chi_{\kappa \neq 0} = AL^2[\ln(L/l_0)]^{-\hat{\eta}'}. \quad (3)$$

The results are given in Table III and we have $\hat{\eta}' > \hat{\eta}$. It is practically difficult to obtain a precise estimate of $\hat{\eta}'$. For reducing uncertainties, we fix l_0 to those produced by the preferred fits of χ_0 to (2). Accordingly, we find $\hat{\eta}' \approx 1.7$ over $\kappa = 1, 1.5, 3$ and 5 (Table IV). From the log-log plot

of $\chi_1 L^{-2}$ versus $\ln(L/l_0)$ in Fig. 2(b) of the main text, we find that the data nearly scale as $\chi_1 L^{-2} \asymp [\ln(L/l_0)]^{-\hat{\eta}'}$ with $\hat{\eta}' \approx 1.59$. As shown in Fig. 2, similar result is found for $\chi_2 L^{-2}$. In short, χ_1 and χ_2 obey the logarithmic scaling formula $\chi_{\kappa \neq 0} \asymp L^2[\ln(L/l_0)]^{-\hat{\eta}'}$, with $\hat{\eta}' \approx 1.6$.

Finally, we analyze the FSS of the helicity modulus Υ , which is defined as [1]

$$\Upsilon = \frac{1}{L^3}(\langle E \rangle - \langle T^2 \rangle), \quad (4)$$

with

$$\begin{aligned} E &= K \sum_{\mathbf{r} \in \text{bulk}} \vec{S}_{\mathbf{r}} \cdot \vec{S}_{\mathbf{r}+\mathbf{e}_x} + K' \sum_{\mathbf{r} \in \text{surfaces}} \vec{S}_{\mathbf{r}} \cdot \vec{S}_{\mathbf{r}+\mathbf{e}_x}, \\ T &= K \sum_{\mathbf{r} \in \text{bulk}} (S_{\mathbf{r}}^a S_{\mathbf{r}+\mathbf{e}_x}^b - S_{\mathbf{r}}^b S_{\mathbf{r}+\mathbf{e}_x}^a) \\ &\quad + K' \sum_{\mathbf{r} \in \text{surfaces}} (S_{\mathbf{r}}^a S_{\mathbf{r}+\mathbf{e}_x}^b - S_{\mathbf{r}}^b S_{\mathbf{r}+\mathbf{e}_x}^a). \end{aligned} \quad (5)$$

Here, a and b denote the two components of the two-dimensional spin vector. \mathbf{e}_x denotes the unit vector along an edge direction of surfaces. The first summation in E and T are over sites in bulk and the second summations run over those on surfaces. For each κ , we perform fits according to the ansatz

$$\Upsilon L = 2\alpha \ln L + A + BL^{-1}, \quad (6)$$

where α is universal and A is non-universal. BL^{-1} stands for finite-size corrections. The results of the fits are summarized in Table V. Notice that the estimates of α for different κ are compatible. By comparing the estimates, our final result is $\alpha = 0.27(2)$.

II. SPECIAL TRANSITION

At the special transition, we analyze the r -dependent behavior of $g(r)$ as well as the FSS of $g(L/2)$, χ_0 , χ_1 and χ_2 . Notice that the transition point $\kappa_c = 0.6222(3)$ and the magnetic renormalization exponent $y_h \approx 1.675(1)$ have been given in literature [2]. The latter relates to the anomalous dimension $\eta \approx 0.650$.

* yjdeng@ustc.edu.cn

† jplv2014@ahnu.edu.cn

As shown in Fig. 3, the r -dependent behavior converges to the power law $g(r) \asymp r^{-\eta}$, with $\eta \approx 0.650$. From Fig. 4, it is confirmed that $g(L/2)$ decays as $g(L/2) \asymp L^{-\eta}$ with $\eta \approx 0.650$, and the magnetic fluctuations χ_0 , χ_1 and χ_2 all scale as $\chi_{\mathbf{k}} \asymp L^{2y_h-2}$ with $y_h \approx 1.675$. Hence, the mag-

netic fluctuations at zero and non-zero Fourier modes share the same leading scaling exponent. This feature is a consequence of the standard scenario for continuous transition, which is not applicable to the extraordinary-log transition.

-
- [1] F. Parisen Toldin, “Boundary critical behavior of the three-dimensional heisenberg universality class,” *Phys. Rev. Lett.* **126**, 135701 (2021), [arXiv:2012.00039 \[cond-mat\]](#).
 [2] Y. Deng, H. W. J. Blöte, and M. P. Nightingale, “Surface and

bulk transitions in three-dimensional $o(n)$ models,” *Phys. Rev. E* **72**, 016128 (2005), [arXiv:cond-mat/0504173 \[cond-mat\]](#).

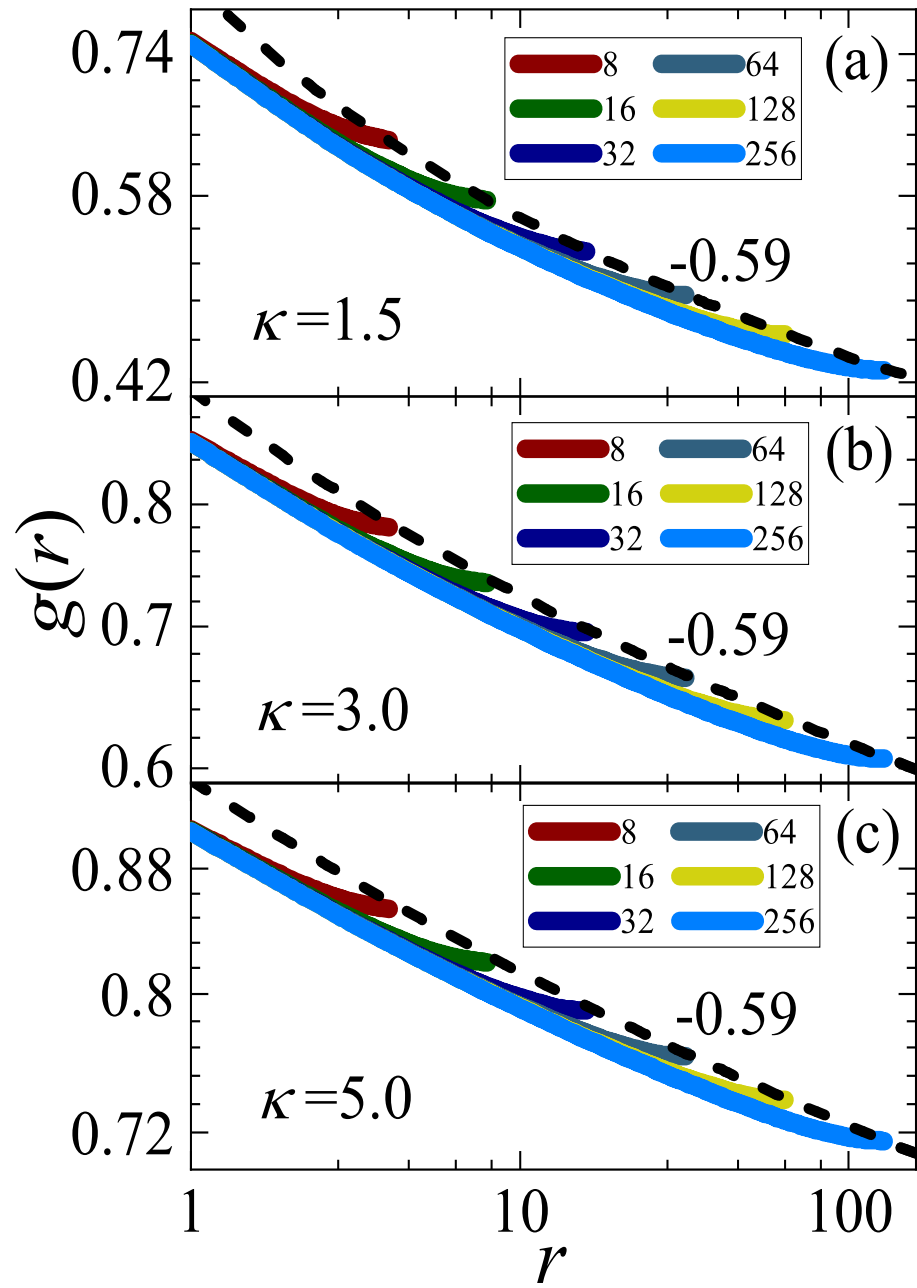


Figure 1. The two-point correlation $g(r)$ for the extraordinary transitions at $\kappa = 1.5, 3,$ and 5 with $L = 8, 16, 32, 64, 128,$ and 256 . The dashed lines denote the logarithmic decaying $[\ln(L/l_0)]^{-0.59}$ in the large-distance limit.

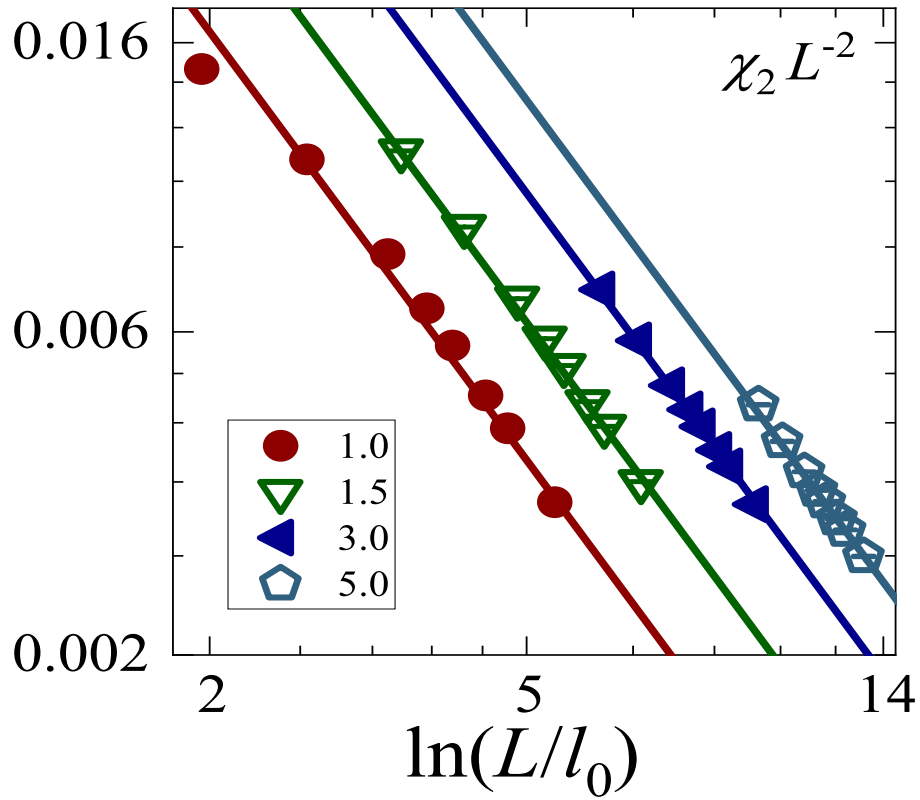


Figure 2. Log-log plot of the scaled magnetic fluctuations $\chi_2 L^{-2}$ versus $\ln(L/l_0)$. Lines have the slope -1.59 and denote the fits to $\chi_2 L^{-2} \asymp [\ln(L/l_0)]^{-\hat{\eta}'}$ with $\hat{\eta}' \approx 1.59$.

Table I. Fits of $g(L/2)$ data to (1).

κ	L_{\min}	χ^2/DF	A	l_0	$\hat{\eta}$
1.0	8	105.10/5	0.853(2)	0.844(6)	0.611(1)
	16	2.91/4	0.822(4)	0.94(1)	0.596(2)
	32	0.66/3	0.813(7)	0.97(2)	0.592(3)
	48	0.58/2	0.81(1)	0.98(4)	0.591(5)
	64	0.58/1	0.81(2)	0.98(6)	0.590(7)
1.5	8	4.39/5	1.385(5)	0.206(3)	0.597(1)
	16	2.63/4	1.395(9)	0.201(5)	0.599(2)
	32	2.41/3	1.39(2)	0.205(10)	0.598(5)
	48	0.04/2	1.36(3)	0.22(2)	0.590(7)
	64	0.03/1	1.35(4)	0.22(2)	0.59(1)
3.0	8	3.39/5	2.29(2)	0.0136(5)	0.582(2)
	16	3.39/4	2.29(3)	0.0136(7)	0.582(4)
	32	2.33/3	2.25(5)	0.015(1)	0.576(7)
	48	2.23/2	2.23(7)	0.015(2)	0.574(10)
	64	1.97/1	2.20(10)	0.017(4)	0.57(1)
5.0	8	4.79/5	3.09(4)	0.00056(4)	0.569(4)
	16	3.10/4	3.15(6)	0.00050(6)	0.575(6)
	32	1.69/3	3.3(1)	0.00041(9)	0.58(1)
	48	0.49/2	3.1(2)	0.0005(2)	0.57(1)
	64	0.38/1	3.2(2)	0.0005(2)	0.58(2)

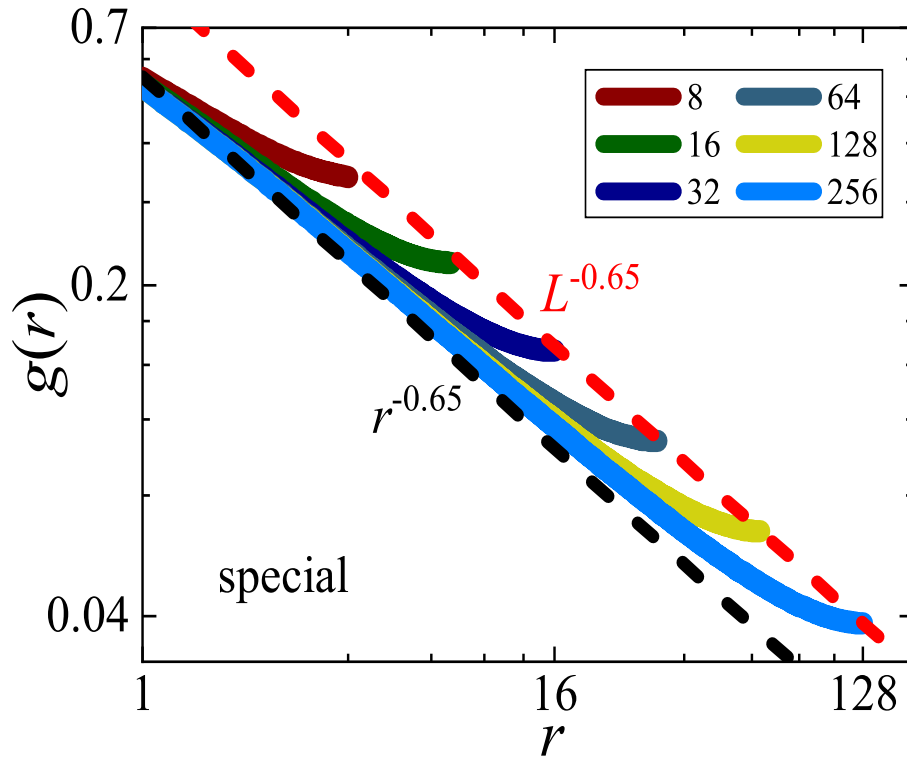


Figure 3. Log-log plot of the two-point correlation $g(r)$ versus r at the special transition $\kappa = 0.6222$.

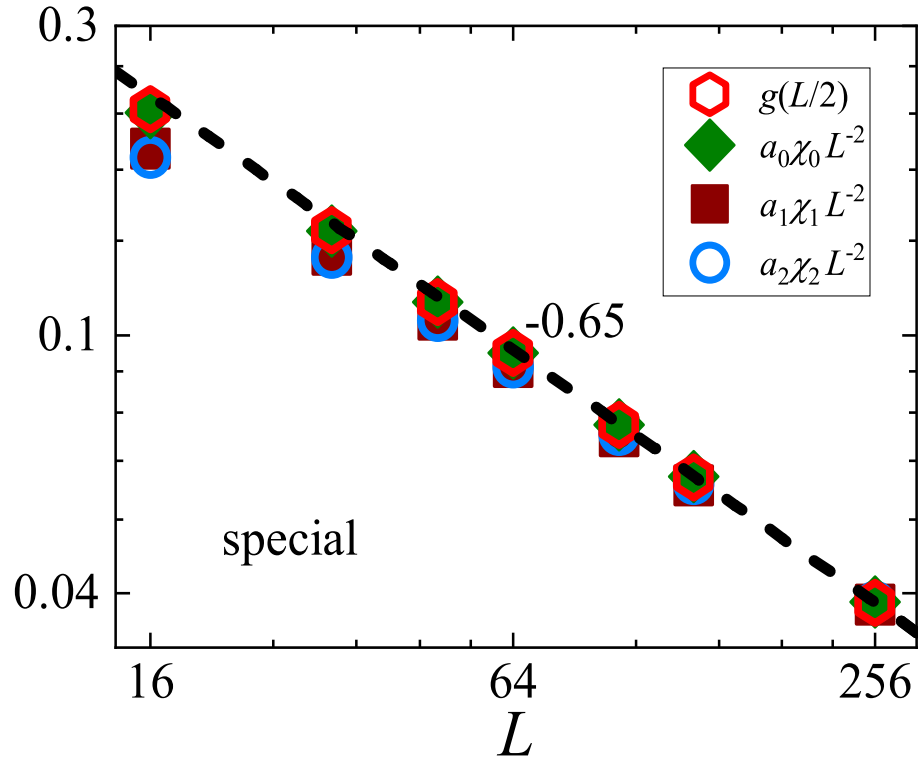


Figure 4. Log-log plot of $g(L/2)$ and scaled magnetic fluctuations $\chi_0 L^{-2}$, $\chi_1 L^{-2}$ and $\chi_2 L^{-2}$ versus L at the special transition point $\kappa = 0.6222$. The parameters a_0 , a_1 and a_2 are used for data collapse. The dashed line has the slope -0.650 and represents the FSS behavior $g(L/2) \asymp L^{-\eta}$ and $\chi_k \asymp L^{2y_h - 2}$ with $\eta = 0.650$ and $y_h = 1.675$.

Table II. Fits of χ_0 to (2).

κ	L_{\min}	χ^2/DF	A	l_0	$\hat{\eta}$
1.0	8	785.73/5	0.936(2)	0.814(5)	0.6495(9)
	16	58.85/4	0.867(3)	1.008(9)	0.619(1)
	32	3.46/3	0.833(5)	1.13(2)	0.603(2)
	48	0.08/2	0.823(7)	1.18(3)	0.598(4)
	64	0.02/1	0.82(1)	1.19(5)	0.597(5)
1.5	8	72.23/5	1.481(4)	0.203(2)	0.622(1)
	16	13.06/4	1.436(7)	0.225(4)	0.611(2)
	32	4.39/3	1.40(1)	0.246(8)	0.602(3)
	48	0.56/2	1.37(2)	0.27(1)	0.594(5)
	64	0.35/1	1.36(3)	0.27(2)	0.592(7)
3.0	8	21.51/5	2.45(2)	0.0121(3)	0.604(2)
	16	9.13/4	2.39(2)	0.0135(6)	0.596(3)
	32	3.39/3	2.32(4)	0.016(1)	0.585(5)
	48	1.15/2	2.26(5)	0.018(2)	0.577(7)
	64	0.92/1	2.23(7)	0.019(3)	0.57(1)
5.0	8	5.20/5	3.30(3)	0.00046(3)	0.588(3)
	16	1.96/4	3.23(5)	0.00052(5)	0.582(4)
	32	1.57/3	3.27(9)	0.00048(8)	0.586(8)
	48	0.12/2	3.2(1)	0.0006(1)	0.58(1)
	64	0.02/1	3.2(2)	0.0005(2)	0.58(2)

Table III. Fits of χ_1 and χ_2 to (3).

Quantity	κ	L_{\min}	χ^2/DF	A	l_0	$\hat{\eta}'$
χ_1	1.0	48	3.79/2	0.35(7)	0.33(6)	2.14(7)
		64	0.18/1	0.24(6)	0.5(1)	2.01(9)
		96	0.00/0	0.2(1)	0.6(4)	1.9(2)
	1.5	48	0.31/2	0.3(1)	0.11(5)	1.9(1)
		64	0.03/1	0.3(1)	0.14(9)	1.8(2)
		96	0.00/0	0.2(3)	0.2(3)	1.8(4)
	3.0	32	2.44/3	1.1(9)	0.002(2)	2.1(2)
		48	1.60/2	3.1(56)	0.0003(8)	2.4(5)
		64	1.04/1	1.0(18)	0.002(5)	2.0(5)
	5.0	32	3.14/3	1.2(23)	0.0000(2)	2.0(5)
		48	1.26/2	0.2(2)	0.003(8)	1.4(4)
		64	1.22/1	0.2(5)	0.001(7)	1.5(7)
χ_2	1.0	48	0.12/2	0.32(7)	0.27(5)	2.36(8)
		64	0.00/1	0.29(9)	0.29(8)	2.3(1)
		96	0.00/0	0.3(2)	0.3(2)	2.3(3)
	1.5	48	0.29/2	0.3(1)	0.07(3)	2.1(1)
		64	0.08/1	0.3(2)	0.09(6)	2.1(2)
		96	0.00/0	0.2(2)	0.1(2)	1.9(5)
	3.0	48	0.55/2	3.8(77)	0.0001(4)	2.6(6)
		64	0.48/1	2.3(59)	0.000(1)	2.5(7)
		96	0.00/0	0.1(4)	0.02(10)	1.7(9)
	5.0	48	3.28/2	0.6(18)	0.0000(2)	2.0(8)
		64	0.15/1	0.04(4)	0.02(7)	1.1(4)
		96	0.00/0	0.2(14)	0.001(8)	1.6(20)

Table IV. Fits of χ_1 and χ_2 to (3), with the parameter l_0 being fixed to those of preferred fits in Table. II.

Quantity	κ	L_{\min}	χ^2/DF	A	l_0	$\hat{\eta}'$
χ_1	1.0	48	72.00/3	0.1023(4)	1.13	1.676(3)
		64	16.07/2	0.1050(6)	1.13	1.693(4)
		96	1.10/1	0.1078(9)	1.13	1.709(6)
		128	0.00/0	0.109(1)	1.13	1.716(8)
	1.5	48	4.66/3	0.174(1)	0.246	1.687(4)
		64	0.91/2	0.176(2)	0.246	1.695(6)
		96	0.03/1	0.178(3)	0.246	1.702(9)
		128	0.00/0	0.179(4)	0.246	1.70(1)
	3.0	48	6.21/3	0.257(4)	0.016	1.635(7)
		64	1.90/2	0.264(5)	0.016	1.647(10)
		96	1.66/1	0.267(9)	0.016	1.65(2)
		128	0.00/0	0.28(1)	0.016	1.67(2)
	5.0	48	1.53/3	0.38(1)	0.00046	1.65(1)
		64	1.25/2	0.38(2)	0.00046	1.65(2)
		96	0.90/1	0.37(2)	0.00046	1.64(2)
		128	0.00/0	0.39(3)	0.00046	1.66(3)
χ_2	1.0	48	102.22/3	0.0684(3)	1.13	1.779(3)
		64	41.47/2	0.0702(4)	1.13	1.796(3)
		96	5.50/1	0.0731(6)	1.13	1.822(6)
		128	0.00/0	0.0747(9)	1.13	1.835(8)
	1.5	48	10.47/3	0.1099(9)	0.246	1.762(4)
		64	3.05/2	0.112(1)	0.246	1.773(6)
		96	0.13/1	0.115(2)	0.246	1.785(9)
		128	0.00/0	0.115(3)	0.246	1.79(1)
	3.0	48	7.09/3	0.156(2)	0.016	1.693(7)
		64	3.00/2	0.160(3)	0.016	1.705(9)
		96	0.00/1	0.167(5)	0.016	1.73(1)
		128	0.00/0	0.167(8)	0.016	1.72(2)
	5.0	48	3.53/3	0.206(6)	0.00046	1.66(1)
		64	1.13/2	0.214(9)	0.00046	1.68(2)
		96	0.00/1	0.20(1)	0.00046	1.66(2)
		128	0.00/0	0.20(2)	0.00046	1.66(3)

Table V. Fits of Υ to (6). In the last column, “-” means that the correction term BL^{-1} is not included.

κ	L_{\min}	χ^2/DF	α	A	B
1.0	8	5.46/4	0.255(3)	0.41(2)	1.60(8)
	16	3.33/3	0.265(7)	0.32(6)	2.2(4)
	32	2.51/2	0.25(2)	0.4(2)	0.8(15)
	48	0.73/1	0.29(3)	0.1(3)	6.4(45)
	32	2.80/3	0.245(4)	0.52(3)	-
	48	2.79/2	0.245(6)	0.52(5)	-
	64	1.64/1	0.252(9)	0.46(8)	-
1.5	8	2.52/5	0.270(2)	1.08(2)	0.82(6)
	16	2.47/4	0.271(7)	1.07(6)	0.9(4)
	32	4.23/4	0.261(3)	1.16(2)	-
	48	0.99/3	0.270(6)	1.09(5)	-
	64	0.23/2	0.276(9)	1.04(8)	-
	96	0.10/1	0.27(2)	1.1(2)	-
	3.0	8	8.21/5	0.278(2)	2.59(2)
16	7.40/4	0.283(6)	2.54(6)	0.8(4)	
32	7.39/3	0.28(2)	2.5(1)	0.9(15)	
48	7.38/2	0.28(3)	2.6(3)	0.3(44)	
16	11.95/5	0.270(1)	2.662(8)	-	
32	7.72/4	0.276(3)	2.62(2)	-	
48	7.38/3	0.278(5)	2.59(4)	-	
64	7.14/2	0.275(8)	2.62(7)	-	
5.0	8	2.23/5	0.276(2)	4.49(2)	0.19(7)
	16	1.73/4	0.281(6)	4.45(6)	0.4(4)
	32	1.17/3	0.27(2)	4.6(2)	-0.7(15)
	8	9.77/6	0.2701(6)	4.538(3)	-
	16	3.19/5	0.273(1)	4.520(8)	-
	32	1.37/4	0.277(3)	4.49(2)	-
	48	1.32/3	0.276(5)	4.50(4)	-
	64	0.76/2	0.271(9)	4.54(8)	-